

Banner appropriate to article type will appear here in typeset article

Passive scalar cascade in the intermediate layer of turbulent channel flow for $Pr \leq 1$

Emanuele Gallorini¹, Shingo Motoki², Genta Kawahara² and Christos Vassilicos¹

¹Univ. Lille, CNRS, ONERA, Arts et Metiers Institute of Technology, Centrale Lille, UMR 9014 - LMFL - Laboratoire de Mécanique des Fluides de Lille - Kampé de Fériet, F-59000 Lille, France

²Graduate School of Engineering Science, University of Osaka, 1-3 Machikaneyama, Toyonaka, Osaka 560-8531, Japan

(Received xx; revised xx; accepted xx)

Similarities and differences between Kolmogorov scale-by-scale equilibria/non-equilibria for velocity and scalar fields are investigated in the intermediate layer of a fully developed turbulent channel flow with a passive scalar/temperature field driven by a uniform heat source. The analysis is based on intermediate asymptotics and direct numerical simulations at different Prandtl numbers lower than unity. Similarly to what happens to the velocity fluctuations, for the fluctuating scalar field Kolmogorov scale-by-scale equilibrium is achieved asymptotically around a length scale r_{min} , which is located below the inertial range. The lengthscale r_{min} and the ratio between the inter-scale transfer and dissipation rates at r_{min} vary following power laws of the Prandtl number, with exponents determined by matched asymptotics based on the hypothesis of homogeneous two-point physics in non-homogeneous turbulence. The interscale transfer rates of turbulent kinetic energy and passive scalar variance are globally similar but show evident differences when their aligned/anti-aligned contributions are considered.

Key words:

1. Introduction

The study of passive scalars representing a dilute diffusive contaminant in a fluid flow or a temperature field with small variations at low Mach numbers, has applications in mixing, combustion, and pollution. It presents complexities that elevate it above being a simple corollary of the fluid flow (Warhaft 2000). Pressure-driven turbulent channel flow (TCF) between two parallel plane walls is a standard test case for turbulence, and this remains true when a passive scalar is present. Several Direct Numerical Simulation (DNS) studies of TCF (Abe *et al.* 2004; Antonia *et al.* 2009; Pirozzoli *et al.* 2016) have highlighted similarities between velocity and passive scalar fields. Despite minor differences relating to forcing and computational setup, these works have shown that both the mean flow and mean scalar profiles have a region of logarithmic dependence on wall normal direction. From the energetic point of view, this region (intermediate layer) is characterized by an approximate balance between turbulence production and dissipation rates for both the turbulent kinetic energy and the

passive scalar variance (Pope 2000). However, the picture appears more complicated when the way turbulent kinetic energy is distributed and transported among different scales and locations is investigated (Cimarelli *et al.* 2013; Gatti *et al.* 2020). Nevertheless, the matched asymptotic analysis of the scale-by-scale turbulent kinetic energy budget in the intermediate layer of a TCF by Apostolidis *et al.* (2023) has shown that a Kolmogorov-type equilibrium between turbulence dissipation and interscale transfer rate is achieved asymptotically (with increasing Reynolds number) only around the Taylor length, and therefore not in the inertial range. These conclusions for a case of a stationary non-homogeneous turbulence agree with the results obtained for non-stationary (freely decaying) homogeneous isotropic turbulence (HIT) far from initial conditions by Lundgren (2002), whose matched asymptotic analysis of the Kármán-Howarth equation leads to the conclusion that the interscale turbulence transfer rate has an extremum at a length scale r_{min} proportional to the Taylor length λ . Wind tunnel data of freely decaying HIT (Obligado & Vassilicos 2019) yield $r_{min} \simeq 1.5\lambda$, and Meldi & Vassilicos (2021) found $r_{min} \simeq 1.12\lambda$ for Taylor length-based Reynolds numbers $Re_\lambda = 10^2$ to 10^6 using an eddy-damped quasinormal Markovian (EDQNM) model of decaying HIT. These works support the idea that a class of turbulent flows exist (including both non-stationary homogeneous and stationary non-homogeneous turbulence) where Kolmogorov-like equilibrium is asymptotically achieved solely in the vicinity of the Taylor length rather than within an inertial range.

But does such a type of localised scale-by-scale budget also hold for a passive scalar field, and if so, around what length-scale? And with what similarities to and differences from the interscale transfer properties of the supporting velocity field? In this paper, we address these questions by studying the interscale transfer rate of passive scalar variance in a TCF, limiting the analysis to the case when the diffusivity of the passive scalar is higher than that of the velocity (i.e., Prandtl number $Pr \leq 1$). Our methods are described in section 2, our results in section 3, and we conclude in section 4.

2. Methods

The present work focuses on turbulent heat and momentum transfer in internally heated channel flow between isothermal impermeable walls. The coordinates x , y , and z represent streamwise, wall-normal and spanwise directions, $\mathbf{u}(\mathbf{x}, t) = (u, v, w)$ is the velocity vector with components in these respective directions, and $\theta(\mathbf{x}, t)$ is the passive temperature field. We use the method of matched asymptotic expansions (Van Dyke 1964) and data from DNS of TCF. The channel has dimensions $L_x \times L_y \times L_z = 2\pi h \times 2h \times \pi h$. The governing equations are the incompressible Navier-Stokes equations for the velocity field and the energy equation, i.e. advection-diffusion equation for the temperature with a uniform internal heat source to maintain constant bulk mean temperature T_b . At the walls ($y = 0$ and $2h$), no-slip boundary conditions apply for the velocity, and a similar Dirichlet condition applies for the temperature. The streamwise and spanwise directions are periodic. The flow is driven by a variable pressure gradient which is adjusted at each timestep to maintain a constant flow rate. In the following, ν and κ are the kinematic viscosity and thermal diffusivity respectively. The flow is characterized by two dimensionless parameters: the bulk Reynolds number $Re_b = 2hU_b/\nu$ and the Prandtl number $Pr = \nu/\kappa$. The present DNS data analysis investigates several cases at $Re_b = 40000$ with different Prandtl numbers $Pr = 1$, $Pr = 0.75$, $Pr = 0.5$, and $Pr = 0.25$. The friction Reynolds number, based on the friction velocity $u_\tau = \sqrt{\bar{\tau}_w/\rho}$ ($\bar{\tau}_w$ is the mean wall shear stress) is $Re_\tau = 1000$. The friction temperature is defined as $\theta_\tau = \kappa dT/dy|_w/u_\tau$, where $dT/dy|_w$ is the wall normal derivative of the mean temperature T at the $y = 0$ wall. The details of the computational procedures and the generation of the database can be found in Motoki *et al.* (2022). The cases with $Pr \neq 1$

are absent in the original database; therefore, additional simulations have been performed for the same configuration using the pseudo-spectral code developed by Luchini & Quadrio (2006). The domain is discretised with $n_x \times n_z = 512 \times 512$ Fourier modes and $n_y = 515$ points in the wall-normal direction, spaced according to a hyperbolic-tangent distribution. The resulting resolution is $\Delta x^+ = 8.2$ and $\Delta z^+ = 4.1$ after dealiasing, while $\Delta y^+ \approx 1$ at the wall and $\Delta y^+ \approx 6.7$ at the centerline, equivalent to similar works on turbulent channel flow at this Reynolds number (Gatti *et al.* 2020), where the superscripts + stand for the normalised length with $\delta_\nu \equiv \nu/u_\tau$. The limited extension of the domain could affect the dynamics of very large-scale structures. However, we expect a limited impact at the scales that we focus on in this study, as confirmed by the agreement between the theoretical predictions and the numerical results in the following section.

We extend the matched asymptotic expansions approach of Apostolidis *et al.* (2023) to passive scalar interscale transfers. They applied this approach to the Kármán-Howarth-Monin-Hill (KMH) equation (Hill 2001) for the turbulent velocity field and we apply it here to the fully generalised Yaglom equation for the passive scalar (Danaila *et al.* 1999) obtained by Hill (2002). These are the budget equations for the second-order structure functions of the velocity and passive scalar respectively. Decomposing the velocity and temperature fields into mean (U, T) and fluctuating (u', θ') fields, these structure functions are $\langle \delta u'^2 \rangle$ and $\langle \delta \theta'^2 \rangle$, where the brackets signify an average; $\delta u' \equiv u'(\mathbf{x} + \mathbf{r}/2, t) - u'(\mathbf{x} - \mathbf{r}/2, t)$ and $\delta \theta' \equiv \theta'(\mathbf{x} + \mathbf{r}/2, t) - \theta'(\mathbf{x} - \mathbf{r}/2, t)$. The centroid \mathbf{x} (components $x_1 \equiv x$, $x_2 \equiv y$, $x_3 \equiv z$) determines spatial location and the separation vector \mathbf{r} (components r_i , $i = 1, 2, 3$) determines length scales. We introduce the additional notation $\mathbf{u}^* \equiv \frac{\mathbf{u}'(\mathbf{x} + \mathbf{r}/2, t) + \mathbf{u}'(\mathbf{x} - \mathbf{r}/2, t)}{2}$ with obvious extension to all other fields, in particular the mean velocity field.

The KMH and fully generalised Yaglom equations are derived directly from the Navier-Stokes and the advection-diffusion equations (Hill 2001, 2002). For the first, we refer the interested reader to Apostolidis *et al.* (2023). The latter reads:

$$\begin{aligned} & \underbrace{\frac{\partial \langle \delta \theta'^2 \rangle}{\partial t}}_{A_{Tt}} + \underbrace{\frac{\partial U_i^* \langle \delta \theta'^2 \rangle}{\partial x_i}}_{\mathcal{T}_{Tm}} + \underbrace{\frac{\partial \langle u_i^* \delta \theta'^2 \rangle}{\partial x_i}}_{\mathcal{T}_T} + 2 \underbrace{\frac{\partial \delta U_i \langle \delta \theta'^2 \rangle}{\partial r_i}}_{\Pi_{Tm}} + \underbrace{\frac{\partial \langle \delta u_i' \delta \theta'^2 \rangle}{\partial r_i}}_{\Pi_T} = \\ & \underbrace{-2 \langle u_i^* \delta \theta' \rangle \frac{\partial \delta T}{\partial x_i}}_{\mathcal{P}_T} - \underbrace{2 \langle \delta u_i' \delta \theta' \rangle \frac{\partial \delta T}{\partial r_i}}_{\mathcal{P}_T} + \underbrace{\frac{\kappa}{2} \frac{\partial^2 \langle \delta \theta'^2 \rangle}{\partial x_i^2}}_{D_{Tx}} + \underbrace{2\kappa \frac{\partial^2 \langle \delta \theta'^2 \rangle}{\partial r_i^2}}_{D_{Tr}} - \underbrace{2(\varepsilon_T^p + \varepsilon_T^m)}_{\varepsilon_T}. \quad (2.1) \end{aligned}$$

In these equations, $\varepsilon_T^p \equiv \kappa \langle \partial \theta'^p / \partial x_j^p \partial \theta'^p / \partial x_j^p \rangle$, $\varepsilon_T^m \equiv \kappa \langle \partial \theta'^m / \partial x_j^m \partial \theta'^m / \partial x_j^m \rangle$ where the p and m superscripts indicate quantities evaluated at $\mathbf{x} + \mathbf{r}/2$ and $\mathbf{x} - \mathbf{r}/2$ respectively. The different terms of equation 2.1 represent different mechanisms: A_{Tt} represent redistribution due to unsteadiness, \mathcal{T}_{Tm} and \mathcal{T}_T are transports in physical space due to mean and fluctuating velocity, Π_{Tm} and Π_T are interscale transfer rates due to mean and fluctuating flow, \mathcal{P}_T is the production rate, D_{Tx} and D_{Tr} are diffusive terms in physical and scale spaces, and ε_T is the turbulent scalar dissipation rate. This work focuses on $Pr \leq 1$.

3. Results

The KMH equation and the generalized Yaglom equation (2.1) can be simplified by tailoring them to the channel flow for which the mean flow is non-zero only in the streamwise direction. Averages are performed in time and along the homogeneous/periodic streamwise

and spanwise directions. Hence, A_{Tt} and \mathcal{T}_m vanish and the remaining terms of the budget depend on (y, \mathbf{r}) . The presence of an approximately logarithmic mean flow in the intermediate layer for $Re_\tau \gg 1$ (Motoki *et al.* 2022) implies that Π_{Tm} is close to zero in the intermediate layer $\delta_v \ll y \ll h$ if $r_2 \ll 2y$. This follows in the same way that Apostolidis *et al.* (2023) showed the equivalent (Π_m) term in the KHMH equation to be about zero in this layer, as $\delta U_2 = \delta U_3 = 0$ and $\delta U_1 = (u_\tau/k) \ln[(1+r_2/y)(1-r_2/y)] \approx 0$ for $r_2/y \ll 1$ (k is the von Kármán coefficient). These authors also showed that the inter-space transfer rate \mathcal{T} and the pressure-velocity term \mathcal{T}_p are also negligible in the intermediate layer. Under the same hypothesis of well-mixed turbulence in this layer when $Re_\tau \gg 1$ and $u_\tau h/\kappa = Re_\tau Pr \gg 1$, we assume that the inter-space transfer rate \mathcal{T}_T is also negligible in this intermediate layer. The low magnitude of $\Xi_t \equiv \Pi_{Tm} + \mathcal{T}_T$ compared to the remaining terms of equation 2.1 is confirmed with DNS data in sub-section 3.3. We therefore have the following simplified balance where every term has been averaged over a sphere in \mathbf{r} space, e.g. $\Pi^v \equiv (6/\pi r^3) \int_{S(r)} \Pi d^3\mathbf{r}$ where $S(r)$ is the sphere of diameter $r \equiv |\mathbf{r}|$:

$$\Pi_T^v \approx \mathcal{P}_T^v + D_{Tx}^v + D_{Tr}^v - \varepsilon_T^v \quad (3.1)$$

valid for $r \ll 2y$ in the intermediate layer $\delta_v \ll y \ll h$. Note that the pressure enters the KHMH equation for the two-point turbulent kinetic energy through a transport term which is negligible in the intermediate layer (Apostolidis *et al.* 2023) so that this KHMH equation features the same qualitative terms as (3.1) in that layer (inter-scale transfer, production, viscous diffusion and dissipation).

3.1. Outer and inner asymptotics

The spherically averaged scalar inter-scale transfer rate is:

$$\Pi_T^v = \frac{3}{2\pi} \int \left\langle \frac{\delta \mathbf{u}' \cdot \hat{\mathbf{r}}}{r} \delta \theta' \delta \theta' \right\rangle d\Omega_r \equiv \frac{S_{T3}(r, y)}{r} \quad (3.2)$$

after use of the Gauss divergence theorem (Ω_r is the solid angle in \mathbf{r} space and $\hat{\mathbf{r}} \equiv \mathbf{r}/r$). The logarithmic law $dT/dy = \theta_\tau/(k_\theta y)$ (where k_θ is a dimensionless coefficient) in the intermediate layer for Re_τ and $Re_\tau Pr$ much larger than 1 (Kader & Yaglom 1972) has been confirmed by (Motoki *et al.* 2022) in their DNS of TCF and implies that the production term takes the form:

$$\mathcal{P}_T^v \approx -\frac{6}{\pi r^3} \frac{\theta_\tau^2 u_\tau}{k_\theta y} \int_0^{r/2} \rho^2 \left[\frac{S_{T12}(\rho, y)}{u_\tau \theta_\tau} - \frac{S_{T1 \times 2}(\rho, y)}{u_\tau \theta_\tau} \right] d\rho \quad (3.3)$$

where:

$$S_{T12}(\rho, y) = 2 \int \langle \delta v' \delta \theta' \rangle \left[1 - \left(\frac{r_y}{2y} \right)^2 \right]^{-1} d\Omega_r \quad (3.4)$$

$$S_{T1 \times 2}(\rho, y) = 2 \int \langle v'^* \delta \theta' \rangle \frac{r_y}{y} \left[1 - \left(\frac{r_y}{2y} \right)^2 \right]^{-1} d\Omega_r. \quad (3.5)$$

Note, however, that our hypothesis that a well-developed logarithmic region exists for T is not supported by DNS data when Pr is low enough (?).

Finally, the molecular diffusion rate can be expressed in terms of $S_{T2} = \int \langle \delta \theta' \delta \theta' \rangle d\Omega_r$ as follows:

$$D_{Tx}^v + D_{Tr}^v = \frac{3\kappa}{\pi r^3} \int_0^{r/2} \rho^2 \frac{d^2 S_{T2}}{dy^2}(\rho, y) d\rho + \frac{3\kappa}{\pi r} \frac{dS_{T2}}{dr}(r, y). \quad (3.6)$$

According to our DNS data, $|S_{T1 \times 2}| \ll |S_{T12}|$, as might be expected. We therefore neglect

$S_{T1 \times 2}$, and the scale-by-scale budget (3.1) can be fully described in terms of the integrals S_{T2} , S_{T3} , S_{T12} and an expression for the scalar dissipation rate ε_T^v .

At this point we invoke the hypothesis of homogeneous two-point physics in non-homogeneous turbulence already introduced by Chen & Vassilicos (2022); Apostolidis *et al.* (2023) for non-homogeneous turbulent velocity fields, but here we apply it to the turbulent scalar field. We therefore hypothesise that, to leading order, $S_{T12}(r, y)$ is the same function of r at different positions y as long as it is scaled by a characteristic temperature $\tau(y)$, velocity $v(y)$ and a length $l_{T12}(Pr, y)$ that are all local in y . We make the same hypothesis for $S_{T2}(r, y)$ and allow for the possibility of a different length $l_{T2}(Pr, y)$:

$$S_{T2}(r, y) = \tau^2(y) a_{T2}(Pr) s_{T2}(r/l_{T2}(Pr, y), y^+) \quad (3.7)$$

$$S_{T12}(r, y) = \tau(y) v(y) a_{T12}(Pr) s_{T12}(r/l_{T12}(Pr, y), y^+) \quad (3.8)$$

where the additional dependence on the local Reynolds number y^+ accounts for higher order corrections to our leading order hypothesis given that we consider asymptotics in the limit $1 \ll y^+ \ll Re_\tau$ with $Pr = O(1)$ kept constant. A dependence on the Prandtl number is retained in the form of dimensionless functions $a_{T2}(Pr)$ and $a_{T12}(Pr)$ to be determined. Moreover, we define the non-dimensional function $s_{T3} = S_{T3}/(\tau^2 v)$. Substituting into equation (3.1) and using the high Re_τ approximation $\varepsilon_T^v \approx u_\tau \theta_\tau^2 / (k_\theta y)$ (Abe & Antonia 2017) in the intermediate/logarithmic layer, we obtain:

$$\begin{aligned} & k_\theta \frac{v \tau^2}{u_\tau \theta_\tau^2} \frac{s_{T3}}{r/y} - \frac{3k_\theta y^2}{\pi r^3 y^+} \frac{a_{T2}}{Pr} \int_0^{r/2} \rho^2 \frac{d^2(\tau/\theta_\tau)^2 s_{T2}}{dy^2} d\rho \\ & - \frac{3k_\theta y^2}{\pi r y^+} \frac{a_{T2}}{Pr} \frac{d(\tau/\theta_\tau)^2 s_{T2}}{dr} \approx -1 - a_{T12} \frac{6}{\pi r^3} \int_0^{r/2} \rho^2 \frac{\tau v}{\theta_\tau u_\tau} s_{T12} d\rho, \end{aligned} \quad (3.9)$$

which is the budget equation for the two-point passive scalar variance in the intermediate region of a turbulent channel flow under the hypothesis of a logarithmic layer for both the mean velocity and scalar fields as might be expected (at least approximately) when $Re_\tau \gg 1$ and $Re_\tau Pr \gg 1$. The hypothesis of homogeneous physics in non-homogeneous turbulence is made both for the smaller scales $r \ll l_{Tn,o}$ where l_{Tn} are outer length scales $l_{Tn,o}$ and for the larger scales $r \gg l_{Tn,i}$ where l_{Tn} are inner length scales $l_{Tn,i}$, with $n = 2$ and 12 .

3.1.1. Outer similarity

We start by obtaining from equation 3.9 the leading order outer scale-by-scale budget equation. For these larger scales we choose outer scalar, velocity and length scales $\tau = \tau_o = \theta_\tau$, $v = v_o = u_\tau$ and $l_{Tn,o} = l_{T_o} = y$. As a consequence, the outer form of equation 3.9 is:

$$\begin{aligned} & k_\theta \frac{s_{T3}}{r/y} - \frac{3k_\theta y^2}{\pi r^3 y^+} \frac{a_{T2}^o}{Pr} \int_0^{r/2} \rho^2 \frac{d^2 s_{T2}}{dy^2} d\rho - \frac{3k_\theta y^2}{\pi r y^+} \frac{a_{T2}^o}{Pr} \frac{ds_{T2}}{dr} \\ & \approx -1 - \frac{6}{\pi r^3} a_{T12}^o \int_0^{r/2} \rho^2 s_{T12} d\rho. \end{aligned} \quad (3.10)$$

This equation suggests outer asymptotic expansions of the form $s_{Tn} = s_{Tn}^{o,0} + \frac{1}{y^+} s_{Tn}^{o,1} + \dots$ for $n = 2, 12$ and 3 in the limit $y^+ \gg 1$, so that its leading order satisfies:

$$k_\theta \frac{s_{T3}^{o,0}}{r/y} \approx -1 - \frac{6}{\pi r^3} a_{T12}^o \int_0^{r/2} \rho^2 s_{T12}^{o,0} d\rho. \quad (3.11)$$

The outer two-point budget is a balance between normalised inter-scale transfer rate on the left hand side and normalised dissipation (-1) and production on the right hand side.

3.1.2. Inner similarity

We now obtain from equation 3.9 the leading order inner scale-by-scale budget equation by concentrating on the physical mechanisms at the smallest scales of the flow. For $r \ll l_{Tn,o}(y)$, we set $\tau^2 = \tau_i^2 = \tau_o^2 g^2(y^+) = \theta_\tau^2 g^2(y^+)$ and we define a length $l_{Ti} = l_{To} f(y^+) = y f(y^+)$ where f and g are a priori unknown decreasing functions with increasing y^+ . It is natural to assume that the inner velocity scale v_i is the same as the one obtained by Apostolidis *et al.* (2023) for the inner scaling of the KHMH equation by a similar approach, and so we adopt $v = v_i = u_\tau (1/y^+)^{1/4}$ which is the Kolmogorov inner velocity scale $u_\eta \equiv (v \varepsilon^v)^{1/4}$. This accounts for our limitation to the $Pr \leq 1$ case for which there are no strong sub-Kolmogorov scalar fluctuations. For the length scales $l_{Tn,i}$, we assume a relation of the form $l_{Tn,i} = c_{Tn}(Pr) l_{Ti}$, where c_{Tn} are dimensionless functions of Prandtl number. Moreover, we assume that the inner dependence on Pr is uniquely represented by the Prandtl relation of $l_{T2,i}$, hence $a_{T2}^i = a_{T12}^i = 1$. As a consequence, the inner form of equation 3.9 is:

$$\begin{aligned} & k_\theta \left(\frac{1}{y^+}\right)^{-1/4} \frac{g^2}{f} \frac{s_{T3}}{r/l_{Ti}} - \frac{3k_\theta}{\pi r^3 y^+} \frac{l_{T2,i}^2}{f^2} \frac{1}{c_{T2}^2 Pr} \int_0^{r/2} \rho^2 \frac{d^2 g^2 s_{T2}}{dy^2} d\rho \\ & - \frac{3k_\theta}{\pi} \frac{1}{c_{T2}^2 Pr} \left(\frac{1}{y^+}\right) \frac{g^2}{f^2} \frac{s'_{T2}}{r/l_{T2,i}} \approx -1 - \frac{6}{\pi r^3} \int_0^{r/2} \rho^2 \left(\frac{1}{y^+}\right)^{1/4} g s_{T12} d\rho \end{aligned} \quad (3.12)$$

where $s'_{T2} = ds_{T2}/d(r/l_{T2,i})$. At inner scales the leading order balance must involve inter-scale energy transfer, molecular diffusion and dissipation without presence of production (second term on the right hand side), which implies $(\frac{1}{y^+})^{-1/4} \frac{g^2}{f} = (\frac{1}{y^+}) \frac{g^2}{f^2} = O(1)$ independent of y^+ . As a result, $g = (y^+)^{-1/4}$ and $f = (y^+)^{-3/4}$, i.e. $\tau_i \sim \theta_\tau (y^+)^{-1/4} \sim \theta_\tau u_\eta / u_\tau$ and $l_{Ti} \sim \eta$ where $\eta \equiv (v^3 / \varepsilon^v)^{1/4}$ is the Kolmogorov length scale. From equation (3.12), it follows that $c_{T2} = 1/\sqrt{Pr}$ so that $l_{T2,i} = c_{T2}(Pr) l_{Ti} \sim \eta / \sqrt{Pr}$ is the Batchelor length scale η_B (Batchelor 1959) which may be interpreted as the distance over which the scalar diffuses by molecular action over a time proportional to the inverse characteristic strain rate $\sqrt{\varepsilon^v / v}$. Note that our analysis leads to the conclusion directly from the two-point budget equation (without use of dimensional analysis) that the inner passive temperature scale τ_i is $\theta_\tau u_\eta / u_\tau$, l_{Ti} is η and $l_{T2,i}$ is η_B .

As the budget equation must also balance beyond the leading order where the production terms must feature, the inner asymptotic expansions must be in terms of powers of $(y^+)^{-1/4} g = (1/y^+)^{1/2}$, i.e. $s_{Tn} = s_{Tn}^{i,0} + (\frac{1}{y^+})^{1/2} s_{Tn}^{i,1} + \dots$ for $n = 2, 12$ and 3 in the limit $y^+ \gg 1$. The leading order inner balance is:

$$k_\theta \frac{s_{T3}^{i,0}}{r/l_{Ti}} - \frac{3k_\theta}{2\pi} \frac{s_{T2}^{i,0}}{r/l_{T2,i}} \approx -1. \quad (3.13)$$

3.2. Matched asymptotics

Matching the leading terms of the outer expansions for $r \gg l_{Tn,i}$ with the leading terms of the inner expansions for $r \ll y$ for S_{T2} at fixed y^+ we obtain:

$$\underbrace{\tau_o^2 a_{T2}^o s_{T2}^{o,0}(r/y, y^+)}_{S_{T2}^{o,0}} = \underbrace{\tau_i^2 s_{T2}^{i,0}(r/\eta_B, y^+)}_{S_{T2}^{i,0}}. \quad (3.14)$$

Using the result $g = (1/y^+)^{1/4}$:

$$a_{T2}^o \left(\frac{r}{y}\right)^n = \left(\frac{1}{y^+}\right)^2 \left(\frac{r}{\eta_B}\right)^n \quad (3.15)$$

leading to $n = 2/3$ and $a_{T2}^o = Pr^{1/3}$. For S_{T12} , as at the largest scales the interscale transfer rate approach zero, equation 3.11 suggests $a_{T12}^o = 1$. By matching outer with inner expansions we obtain:

$$\underbrace{\tau_o v_o s_{T12}^{o,0}(r/y, y^+)}_{S_{T12}^{o,0}} = \underbrace{\tau_i v_i s_{T12}^{i,0}(r/l_{T12,i}, y^+)}_{S_{T12}^{i,0}}, \quad (3.16)$$

leading to:

$$\left(\frac{r}{y}\right)^n = \left(\frac{1}{y^+}\right)^2 \left(\frac{r}{\eta c_{T12}}\right)^n \quad (3.17)$$

resulting in $n = 2/3$ and $c_{T12}^i = 1$. The leading orders are $S_{T2}^0 \sim Pr^{1/3}(\varepsilon_T^v/\varepsilon^v)(\varepsilon^v r)^{2/3}$ (similar to the Corrsin-Obukhov scalar spectrum for homogeneous turbulence, see Batchelor (1959), but with an additional $Pr^{1/3}$ prefactor) and $S_{T12}^0 \sim (\varepsilon_T^v/\varepsilon^v)^{1/2}(\varepsilon^v r)^{2/3}$ in the intermediate range $y_i \ll r \ll y$. It also follows that the inner scalings of S_{T2} and S_{T12} are, respectively, $\theta_\tau^2 u_\tau^{-2} u_\eta^2 F(r/l_{T2,i})$ and $\theta_\tau u_\tau^{-1} u_\eta^2 G(r/l_{Ti})$ (F, G dimensionless functions).

The scalar inter-scale transfer rate Π_T^v is obtained from S_{T3} for which we use the leading order outer and inner balances (3.11) and (3.13). The former leads to $S_{T3}^{o,0} \approx -\varepsilon_T^v r [1 - A(r/y)^{2/3}]$ whilst the latter leads to $S_{T3}^{i,0} \approx -\varepsilon_T^v r [1 - B(r/\eta_B)^{-4/3}]$ where A and B are dimensionless constants. Following the rule of van Dyke (Van Dyke 1964), the composite leading order is $S_{T3}^{o,0}$ plus $S_{T3}^{i,0}$ minus their common part which is $-\varepsilon_T^v r$. Hence:

$$\Pi_T^v \approx -\varepsilon_T^v \left(1 - A(r/y)^{2/3} - \frac{B}{Pr^{2/3}}(r/\eta)^{-4/3}\right). \quad (3.18)$$

Equation 3.18 implies the existence of a scale $r = r_{min}$ where $|\Pi_T^v|/\varepsilon_T^v$ is maximal: r_{min} and the value $(\Pi_T^v/\varepsilon_T^v)_{min}$ of Π_T^v/ε_T^v at $r = r_{min}$ are (λ being the Taylor length)

$$r_{min} \sim \sqrt{\frac{\delta_v y}{Pr^{2/3}}} \sim \frac{\lambda}{Pr^{1/3}} = \lambda_T \quad (3.19)$$

$$1 + (\Pi_T^v/\varepsilon_T^v)_{min} \sim (Pr^{2/3} y^+)^{-1/3} \sim Pr^{-2/9} Re_\lambda^{-2/3}. \quad (3.20)$$

Similarly to the conclusion of Apostolidis *et al.* (2023) for the velocity field, in the TCF's intermediate region, a Kolmogorov equilibrium $\Pi_T^v = -\varepsilon_T^v$ can be reached asymptotically only around λ_T , with systematic departures caused by production at larger scales (term $A(r/y)^{2/3}$ in (3.18)) and by molecular diffusion at smaller scales (term $B(r/\eta_B)^{-4/3}$ in equation (3.18)).

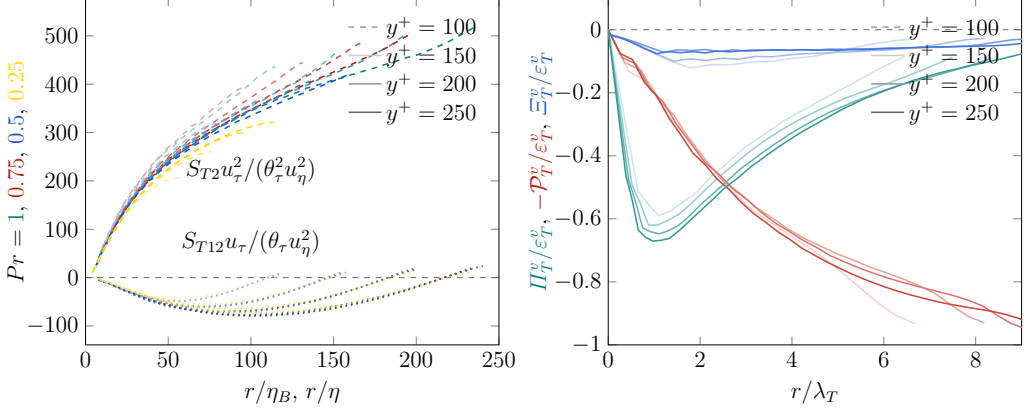


Figure 1: Left panel: $S_{T2}u_{\tau}^2/(\theta_{\tau}^2u_{\eta}^2)$ and $S_{T12}u_{\tau}/(\theta_{\tau}u_{\eta}^2)$ as functions of r/η_B and r/η respectively. Right panel: II_T^y/ϵ_T^y (green lines), P_T^y/ϵ_T^y (red lines), and transport terms $\Xi_T^y/\epsilon_T^y = (II_{Tm}^y + \mathcal{T}_T^y)/\epsilon_T^y$ (blue lines) for $Pr = 1$. Wall-normal distance is increased from light to dark colours.

3.3. Verification of the theory with the DNS data

In this section, we use TCF DNS data to verify the theoretical conclusions in sections 3.1 and 3.2. The top-left panel of figure 1 verifies the validity of the derived inner scalings $S_{T2} = \theta_{\tau}^2 u_{\tau}^{-2} u_{\eta}^2 F(r/\eta_B)$ and $S_{T12} = \theta_{\tau} u_{\tau}^{-1} u_{\eta}^2 G(r/\eta)$ by reporting how $S_{T2}u_{\tau}^2/(\theta_{\tau}^2u_{\eta}^2)$ and $S_{T12}u_{\tau}/(\theta_{\tau}u_{\eta}^2)$ evolve as functions of r/η_B and r/η respectively. The collapse of the two sets of curves at small scales is not perfect but satisfactory if we consider that our DNS values of Re_{τ} and $Re_{\tau}Pr$ are not as large as might be required by our asymptotic analysis.

The right panel of figure 1 represents different terms in the balance equation 2.1 integrated over the volume of a sphere of radius $r/2$, at different wall-normal locations. The results for the case $Pr = 1$ are reported for conciseness, but similar behaviour is observed for our other Pr values. Green lines represent inter-scale transfer rate and red lines represent production rate, both normalised by the volume integral of the two-point dissipation rate. In blue, we report the terms neglected in the budget equation 3.1 to confirm that they are small: it is worth noticing that their value is not zero, indicating that due to the limited value of Re_{τ} these redistribution processes are low but still weakly active.

The qualitative behavior of the different terms of the budget equations is similar for the velocity (Apostolidis *et al.* 2023) and the passive scalar. The production rate increases as r/λ_T increases above 1: at the smallest scales below λ_T , the production rate is small, but it is present and non-negligible at all scales larger than λ_T reaching, at the largest scales, the one-point log-layer equilibrium $\mathcal{P}_T^y \approx \epsilon_T^y$.

The inter-scale transfer rate is negative at all scales indicating a cascade from large to small scales on average. As predicted in the previous sub-section, the minima of II_T^y/ϵ_T^y happen at similar values of r/λ_T for all y^+ , and $(II_T^y/\epsilon_T^y)_{min}$ decreases as y^+ and local Re_{λ} increase. The production-generated systematic departure from Kolmogorov two-point equilibrium is present throughout the inertial range, i.e. at all scales larger than λ_T .

The theoretical relations (3.19)-(3.20) for the passive scalar stemming from our matched asymptotic expansion are quantitatively verified in figure 2 for different Pr . The left panels show the length-scale r_{min} of the minimum of the ratio between the inter-scale transfer and dissipation rates versus y^+ . In the top left panel, r_{min} is normalised with λ , in the bottom left panel with λ_T . For all cases, r_{min} collapses once scaled with $Pr^{-1/3}$, i.e. as r/λ_T . The minimum is at an almost constant value of $r/\lambda_T \sim 1$ for all y^+ in the intermediate

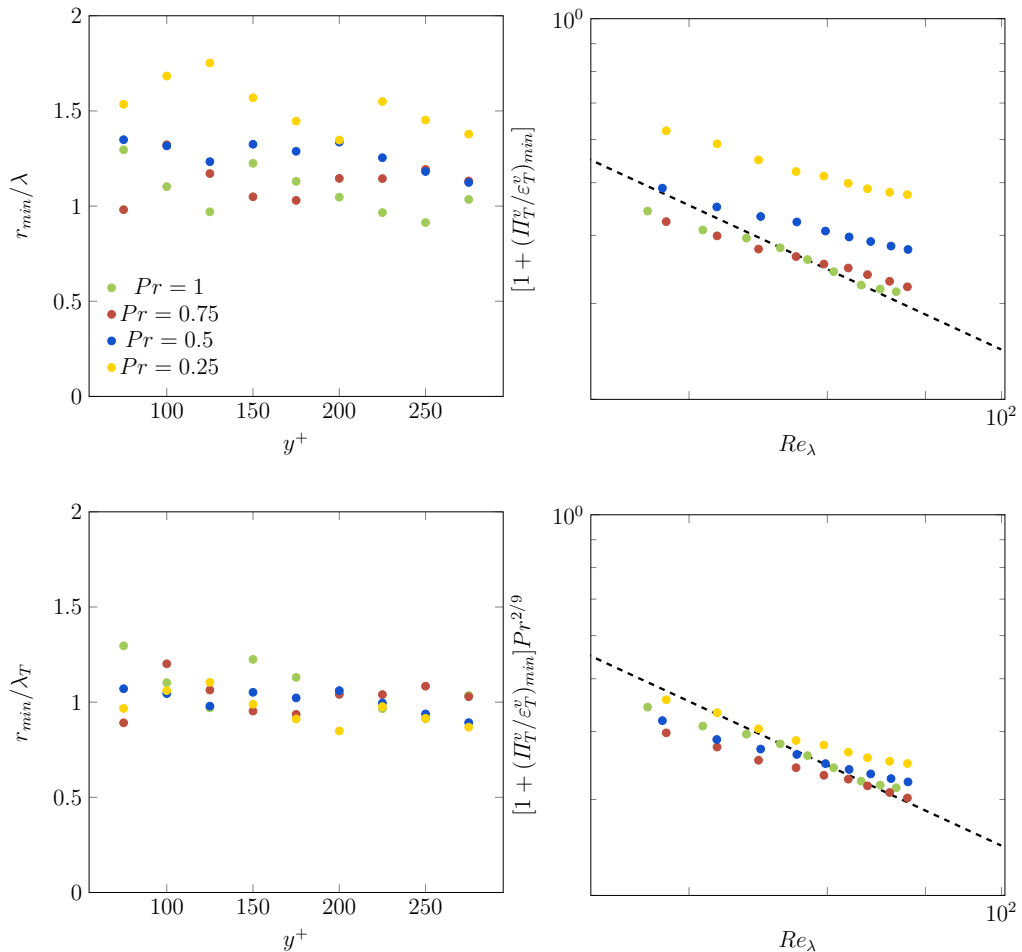


Figure 2: Scale r_{min} of Π_T^v/ε_T^v minima as a function of wall distance y^+ (left) and values of $1 + (\Pi_T^v/\varepsilon_T^v)_{min}$ as a function of Re_λ (right). Top panels: quantities not scaled with Pr . Bottom panels: quantities scaled with Pr . The dashed line in the right panels is proportional to $Re_\lambda^{-2/3}$.

layer and all our Pr values in agreement with (3.19). The right panels of figure 2 show $1 + (\Pi_T^v/\varepsilon_T^v)_{min}$ versus Re_λ (which varies with y^+). Considering the relatively low values of Re_λ , the data collapse quite well on the line $Re_\lambda^{-2/3}$ once multiplied by $Pr^{2/9}$ as per our prediction (3.20). The turbulent Reynolds numbers Re_λ are not high, and their range is narrow in the intermediate layer at $Re_\tau = 1000$. Due to the limited Reynolds number and the narrow dynamical range, deviations from the theoretical model are to be expected. Similar deviations were also pointed out by Apostolidis *et al.* (2023) at $Re_\tau = 1000$, who also observed their reduction at $Re_\tau = 2000$. The departure from this theoretical prediction increases as Pr decreases. Indeed, the theoretical prediction is made for $Re_\tau \gg 1$ and $Re_\tau Pr \gg 1$ and the condition $Re_\tau Pr \gg 1$ progressively weakens with decreasing Pr for a given Re_τ (as is the case in figure 2). The logarithmic region also becomes less well-defined as Pr decreases (?). The best DNS agreement with the theoretical scaling (3.20) occurs for $Pr = 1$ which is the case where $Re_\tau Pr$ is the highest in our DNS data. As Pr decreases while keeping Re_τ constant, the properties of the scalar intermediate layer which lead to

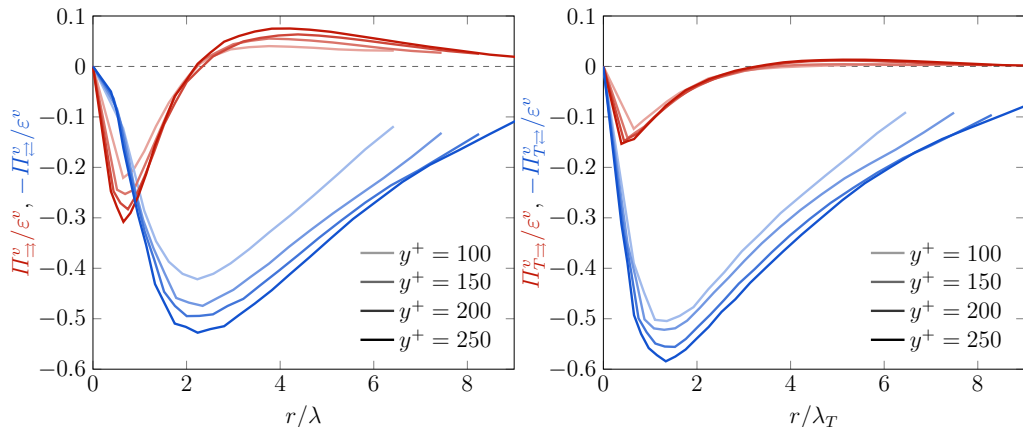


Figure 3: Decomposition of the inter-scale transfer rate into anti-aligned (blue lines) and aligned (red lines) contributions for $Pr = 1$. Left panel: Velocity; Right panel: Temperature.

our theoretical predictions deteriorate, namely, the assumed scaling of the turbulent scalar dissipation rate ε_T^v and the presence of a well-developed approximate log layer for the passive scalar. Finally, Re_λ increases as y^+ increases and as y^+ increases we move towards the edge and out of the intermediate layer where the theoretical predictions are designed for.

3.4. Inter-scale transfer rate analysis

Given that the previous sub-section's results for the passive scalar fluctuations are similar to those of Apostolidis *et al.* (2023) for the velocity fluctuations in the same flow, this section focuses on a more detailed comparison between inter-scale transfer of turbulent energy and turbulent scalar variance. In figure 3 we concentrate on our highest $Re_\tau Pr$ value (i.e. $Pr = 1$) and plot inter-scale transfer rates decomposed into aligned and anti-aligned contributions for the velocity (left panels) and temperature (right panels). Aligned and anti-aligned contributions arise from the following decomposition introduced by Apostolidis *et al.* (2023) for the inter-scale turbulent energy transfer rate Π^v and explicitly given here for Π_T^v :

$$\Pi_T^v = \Pi_{T\rightleftharpoons}^v + \Pi_{T\Leftarrow}^v = \frac{3}{4\pi} \int d\Omega \left\langle \frac{\delta \mathbf{u}' \cdot \hat{\mathbf{r}}}{r} \delta \theta' \delta \theta' \right\rangle_{\rightleftharpoons} + \frac{3}{4\pi} \int d\Omega \left\langle \frac{\delta \mathbf{u}' \cdot \hat{\mathbf{r}}}{r} \delta \theta' \delta \theta' \right\rangle_{\Leftarrow} \quad (3.21)$$

where the conditional average $\langle \dots \rangle_{\rightleftharpoons}$ is taken over pairs of points where fluctuating velocities are aligned, i.e. $\mathbf{u}'(\mathbf{x} + \mathbf{r}/2) \cdot \mathbf{u}'(\mathbf{x} - \mathbf{r}/2) > 0$, and the conditional average $\langle \dots \rangle_{\Leftarrow}$ is taken over pairs of points where fluctuating velocities are anti-aligned, i.e. $\mathbf{u}'(\mathbf{x} + \mathbf{r}/2) \cdot \mathbf{u}'(\mathbf{x} - \mathbf{r}/2) < 0$. Both Π^v and Π_T^v involve the multiplication of the second-order structure functions (respectively of velocity and temperature) and the projected velocity difference $\delta \mathbf{u}' \cdot \hat{\mathbf{r}}$. The local sign of the velocity and temperature cascades is fully determined by $\delta \mathbf{u}' \cdot \hat{\mathbf{r}}$, with compressions ($\delta \mathbf{u}' \cdot \hat{\mathbf{r}} < 0$) causing forward cascades and stretchings ($\delta \mathbf{u}' \cdot \hat{\mathbf{r}} > 0$) causing inverse cascades. Clearly, the local sign of the cascade is not enough to compute its average value which stems from weighted averaging as per the above equation. Note that both aligned and anti-aligned components can involve both compressions and stretchings and therefore result in either a forward or inverse cascade component. Our results for the scalar fluctuations and those of Apostolidis *et al.* (2023) for the velocity fluctuations show that Π_T^v and Π^v have similar evolutions with r/λ_T and r/λ respectively, and that they are both negative at all the scales, meaning that local compressions dominate over local stretchings on average. In

figure 3 we compare how aligned and anti-aligned pairs of velocity contribute to the cascade for the velocity and the cascade for the scalar. The anti-aligned components decrease and reach a minimum at a scale $r > r_{min}$, and then increase towards zero as expected since production balances dissipation at the largest scales. They dominate the inter-scale transfer rates at scales $r > r_{min}$ and show similar evolutions with $r/\lambda-r/\lambda_T$ for $\delta\mathbf{u}'\delta\mathbf{u}'$ and $\delta\theta'\delta\theta'$. The aligned contributions to the inter-scale transfer rate also show similar evolutions with $r/\lambda-r/\lambda_T$ for $\delta\mathbf{u}'\delta\mathbf{u}'$ and $\delta\theta'\delta\theta'$, reaching a minimum at a scale $r < r_{min}$ for both the scalar and the velocity cases. Despite these similar evolutions, the aligned contributions are clearly different as their magnitude is significantly lower for the temperature than for the velocity fields. Furthermore, the peak value of $\Pi_{\rightleftharpoons}^v/\varepsilon^v$ appears to coincide in r with the zero value of $\Pi_{\rightleftharpoons}^v/\varepsilon^v$ (where ε^v is the sphere-averaged turbulence dissipation rate). If this coincidence (3) persists as $Re_\tau \rightarrow \infty$ then the intermediate asymptotic theory of Apostolidis *et al.* (2023) would imply that $\Pi_{\rightleftharpoons}^v/\varepsilon^v$ tends to -1 in that limit. However, the peak value of $\Pi_{T\rightarrow}^v/\varepsilon_T^v$ does not coincide in r with the zero value of $\Pi_{T\rightarrow}^v/\varepsilon_T^v$ as clearly seen in 3. If this lack of coincidence persists as $Re_\tau \rightarrow \infty$ then (3.20) would imply that $\Pi_{T\rightarrow}^v/\varepsilon_T^v$ does not tend to -1 in that limit. Even though the overall physical process determining the direction of the cascade is the same for velocity and temperature (compressions and stretchings via $\delta\mathbf{u}' \cdot \mathbf{n}$), there are significant differences arising from whether compressions and stretchings result from aligned or anti-aligned fluctuating velocities. The explanation of these differences will require a dedicated future study which may need to consider the underlying flow structure of the turbulence, for example, in terms of ejections and sweeps.

4. Conclusions

We performed a scale-by-scale analysis of passive scalar fluctuations in the intermediate layer of a fully developed turbulent channel flow to assess the presence or absence of a Kolmogorov-like equilibrium. The turbulent channel flow analysis of Apostolidis *et al.* (2023) has had to be non-trivially extended to account for a passive scalar with Prandtl number $Pr \leq 1$ in the limit $Re_\tau Pr \gg 1$. It transpired from our hypothesis of homogeneous physics in non-homogeneous turbulence combined with the Navier-Stokes equation that the scalar fluctuations' inner length scale is the Batchelor length even though the turbulence in the channel flow's intermediate layer is not homogeneous down to very small scales. Indeed, the Batchelor length was originally introduced by Batchelor (1959) for homogeneous turbulence, yet two-point turbulent scalar production, and therefore non-homogeneity, in the channel flow's intermediate layer are significant down to length-scales as small as $\lambda_T = \lambda Pr^{-1/3}$. It also follows from our analysis that the scalar field's average interscale transfer rate is negative (forward cascade on average) and maximal at a specific length-scale $r_{min} \sim \lambda_T$. The tendency towards a Kolmogorov equilibrium between scalar interscale transfer rate and scalar dissipation rate is achieved asymptotically ($Re_\tau \rightarrow \infty$) at that length scale only, and systematic departures from this equilibrium are present and increase with length-scale throughout the inertial range because of the presence of two-point scalar turbulence production. These theoretical arguments have been verified with DNS of turbulent velocity and scalar fields in channel flow at different Prandtl numbers $Pr = 1, 0.75, 0.5, \text{ and } 0.25$. Good agreement has been found between the hypotheses and the predictions on the one hand, and the DNS data on the other. Even though the aforementioned results and respective ones in Apostolidis *et al.* (2023) demonstrate a close analogy between the interscale transfer properties of turbulent velocity and scalar fields in the intermediate layer of turbulent channel flow, there are some significant differences between them. Whilst the interscale transfer rates Π^v (for the fluctuating velocity) and Π_T^v (for the fluctuating scalar) have similar evolutions

with length-scale r , the contributions from aligned and anti-aligned pairs of fluctuating velocities differ for Π^v and Π_r^v .

Declaration of Interests

The authors report no conflict of interest.

Acknowledgments

J.C.V. acknowledges funding by the European Union (ERC Advanced Grant NoStaHo, project number 101054117). Views and opinions expressed are, however, those of the author(s) only and do not necessarily reflect those of the European Union or the European Research Council. Neither the European Union nor the granting authority can be held responsible for them. This project was provided with computing HPC and storage resources by GENCI at CINES thanks to the grant 2025-A0182A01741 on the supercomputer Adastra's GENOA partition .

REFERENCES

- ABE, H. & ANTONIA, R. A. 2017 Relationship between the heat transfer law and the scalar dissipation function in a turbulent channel flow. *Journal of Fluid Mechanics* **830**, 300–325.
- ABE, H., KAWAMURA, H. & MATSUO, Y. 2004 Surface heat-flux fluctuations in a turbulent channel flow up to $Re_\tau = 1020$ with $Pr = 0.025$ and 0.71 . *International Journal of Heat and Fluid Flow* **25** (3), 404–419.
- ANTONIA, R. A., ABE, H. & KAWAMURA, H. 2009 Analogy between velocity and scalar fields in a turbulent channel flow. *Journal of Fluid Mechanics* .
- APOSTOLIDIS, A., LAVAL, J. P. & VASSILICOS, J. C. 2023 Turbulent cascade in fully developed turbulent channel flow. *Journal of Fluid Mechanics* **967**, A22.
- BATCHELOR, G. K. 1959 Small-scale variation of convected quantities like temperature in turbulent fluid Part I. General discussion and the case of small conductivity. *Journal of Fluid Mechanics* **5** (1), 113–133.
- CHEN, J. G. & VASSILICOS, J. C. 2022 Scalings of scale-by-scale turbulence energy in non-homogeneous turbulence. *Journal of Fluid Mechanics* **938**, A7.
- CIMARELLI, A., DE ANGELIS, E. & CASCIOLA, C. M. 2013 Paths of energy in turbulent channel flows. *Journal of Fluid Mechanics* **715**, 436–451.
- DANAÏLA, L., ANSELMET, F., ZHOU, T. & ANTONIA, R. A. 1999 A generalization of Yaglom's equation which accounts for the large-scale forcing in heated decaying turbulence. *Journal of Fluid Mechanics* **391**, 359–372.
- GATTI, D., CHIARINI, A., CIMARELLI, A. & QUADRIO, M. 2020 Structure function tensor equations in inhomogeneous turbulence. *Journal of Fluid Mechanics* **898**, A5–33.
- HILL, R. J. 2001 Equations relating structure functions of all orders. *Journal of Fluid Mechanics* **434**, 379–388.
- HILL, R. J. 2002 Structure-function equations for scalars. *Physics of Fluids* **14** (5), 1745–1756.
- KADER, B. A & YAGLOM, A. M 1972 Heat and mass transfer laws for fully turbulent wall flows. *International Journal of Heat and Mass Transfer* **15** (12), 2329–2351.
- LUCHINI, P. & QUADRIO, M. 2006 A low-cost parallel implementation of direct numerical simulation of wall turbulence. *Journal of Computational Physics* **211** (2), 551–571.
- LUNDGREN, T. S. 2002 Kolmogorov two-thirds law by matched asymptotic expansion. *Physics of Fluids* **14** (2), 638–642.
- MELDI, M. & VASSILICOS, J. C. 2021 Analysis of Lundgren's matched asymptotic expansion approach to the Kármán-Howarth equation using the eddy damped quasinormal Markovian turbulence closure. *Physical Review Fluids* **6** (6), 064602.
- MOTOKI, S., TSUGAWA, K., SHIMIZU, M. & KAWAHARA, G. 2022 The ultimate state of turbulent permeable-channel flow. *Journal of Fluid Mechanics* **931**, R3.
- OBLIGADO, M. & VASSILICOS, J. C. 2019 The non-equilibrium part of the inertial range in decaying homogeneous turbulence. *Europhysics Letters* **127** (6), 64004.

- PIROZZOLI, S., BERNARDINI, M. & ORLANDI, P. 2016 Passive scalars in turbulent channel flow at high Reynolds number. *Journal of Fluid Mechanics* **788**, 614–639.
- POPE, S. B. 2000 *Turbulent Flows*. Cambridge University Press, Cambridge.
- VAN DYKE, M. D. 1964 *Perturbation methods in fluid mechanics*. Academic Press, New York.
- WARHAFT, Z. 2000 Passive Scalars in Turbulent Flows. *Annual Review of Fluid Mechanics* **32**, 203–240.